

1 EyeLayer: Integrating Human Attention Patterns into LLM-Based 2 Code Summarization

3 Anonymous Author(s)

4 Abstract

5 Code summarization is the task of generating natural language
6 descriptions of source code, which is critical for software compre-
7 hension and maintenance. While large language models (LLMs)
8 have achieved remarkable progress on this task, an open question
9 remains: can human expertise in code understanding further guide
10 and enhance these models? We propose EyeLayer, a lightweight
11 attention-augmentation module that incorporates human eye-gaze
12 patterns, as a proxy of human expertise, into LLM-based code sum-
13 marization. EyeLayer models human attention during code reading
14 via a Multimodal Gaussian Mixture, redistributing token embed-
15 dings based on learned parameters (μ_i, σ_i^2) that capture where and
16 how intensively developers focus. This design enables learning
17 generalizable attention priors from eye-tracking data and incor-
18 porating them into LLMs seamlessly, without disturbing existing
19 representations. We evaluate EyeLayer across diverse model fam-
20 ilies (i.e., LLaMA-3.2, Qwen3, and CodeBERT) covering different
21 scales and architectures. EyeLayer consistently outperforms strong
22 fine-tuning baselines across standard metrics, achieving gains of
23 up to 13.17% on BLEU-4. These results demonstrate that human
24 gaze patterns encode complementary attention signals that enhance
25 the semantic focus of LLMs and transfer effectively across diverse
26 models for code summarization.

31 Keywords

32 Code Summarization, Human Factors in Software Engineering,
33 Human-centered AI for Software Engineering

35 ACM Reference Format:

36 Anonymous Author(s). 2018. EyeLayer: Integrating Human Attention Pat-
37 terns into LLM-Based Code Summarization. In *Proceedings of Make sure*
38 *to enter the correct conference title from your rights confirmation email*
39 *(Conference acronym 'XX)*. ACM, New York, NY, USA, 12 pages. <https://doi.org/XXXXXXXXXXXXXX>

41 1 Introduction

42 Software documentation is an essential bridge between code imple-
43 mentation and developer understanding, with code summarization
44 facilitating efficient program comprehension [1, 46]. As modern
45 software systems become increasingly complex, quickly grasping
46 code functionality through concise summaries is critical for main-
47 tenance and evolution. Consequently, automatically generating

49 Permission to make digital or hard copies of all or part of this work for personal or
50 classroom use is granted without fee provided that copies are not made or distributed
51 for profit or commercial advantage and that copies bear this notice and the full citation
52 on the first page. Copyrights for components of this work owned by others than the
53 author(s) must be honored. Abstracting with credit is permitted. To copy otherwise, or
54 republish, to post on servers or to redistribute to lists, requires prior specific permission
55 and/or a fee. Request permissions from permissions@acm.org.

55 *Conference acronym 'XX, Woodstock, NY*

56 © 2018 Copyright held by the owner/author(s). Publication rights licensed to ACM.

57 ACM ISBN 978-1-4503-XXXX-X/2018/06

58 <https://doi.org/XXXXXXXXXXXXXX>

59 high-quality summaries has become a central challenge in software
60 engineering [24, 37].

61 Recent advances in large language models (LLMs) have demon-
62 strated remarkable capabilities in code-related tasks, particularly in
63 code summarization [11, 21, 46]. While these models have achieved
64 good performance by learning from vast corpora of code–summary
65 pairs, there remains a gap in generating human-aligned summaries
66 that capture the information humans actually focus on during
67 code comprehension [2, 5]. Meanwhile, when developers com-
68 prehend code to formulate summaries, their attention patterns re-
69 veal how they selectively allocate focus across different parts of
70 the code [24, 40]. In previous software engineering research, eye-
71 tracking studies have been widely used to extract developers’ at-
72 tention patterns which is a promising proxy for their cognitions
73 during programming activities [39, 41, 42]. This motivates a key
74 question: **can incorporating human attention signals further
75 enhance LLM-based code summarization?**

76 The most recent research has attempted to guide AI model devel-
77 opment leveraging developers’ attention patterns and demonstrated
78 promising benefits of such guidance. EyeTrans [55] for the first time
79 integrated eye-gaze signals into a single Transformer block for code
80 summarization, achieving up to 6.39% improvement. However, it
81 remains unknown whether human attention can actually enhance
82 modern LLMs, which differ substantially in scale, architecture, and
83 optimization dynamics. This uncertainty limits their potential im-
84 pact on real-world applications.

85 To bridge the gap between human and LLM attention mecha-
86 nisms, we propose **EyeLayer**, a lightweight architectural module
87 that integrates human eye-gaze data into LLM-based code sum-
88 marization. Our approach is grounded in a key insight: during code
89 comprehension, programmers naturally focus their attention un-
90 evenly across the code, concentrating intensively on semantically
91 critical regions while peripherally attending to contextual elements.
92 EyeLayer models this distributional attention as a transferable prior,
93 learned from a curated eye-tracking corpus of 27 professional de-
94 velopers [55], which captures how human gaze behavior reflects
95 semantic importance during real code comprehension. It employs
96 a **Multimodal Gaussian Mixture** to redistribute each code em-
97 bedding based on learned parameters (μ_i, σ_i^2), which encode both
98 the intensity and spread of human attention. Integrated into the
99 supervised fine-tuning process, EyeLayer leverages these human-
100 derived priors to improve how pretrained models allocate focus
101 across code tokens without altering the original model architec-
102 ture. Despite being trained on a small but cognitively grounded
103 dataset, EyeLayer generalizes effectively to large-scale LLMs, show-
104 ing that even limited human attention data can yield measurable
105 improvements.

106 Functionally, EyeLayer serves as a recommendation system for
107 code embedding redistribution: for each code embedding, it predicts
108 a small set of Gaussian modes that recommend how its representa-
109 tion should be redistributed. This mechanism allows the model to

compose fine-grained and global focus patterns, analogous to personalized recommendation in representation space. By decoupling gaze-informed redistribution from the model’s intrinsic attention weights, EyeLayer learns generalizable attention priors from sparse eye-tracking data and transfers them to unseen code. Incorporated within LLMs, it preserves pretrained representations while infusing human-like focus behavior directly into the attention redistribution process.

We evaluate EyeLayer across five models spanning different scales and architectures: CodeBERT (125M) [14], LLaMA-3.2-1B/3B-Instruct [18], and Qwen3-1.7B/4B-base [48]. All EyeLayer-augmented models are compared against strong supervised fine-tuned baselines trained on identical code summarization data (CodeXGLUE [22, 29]) but without eye-tracking integration, isolating the contribution of human attention signals. Evaluation uses four widely-adopted metrics capturing lexical overlap (BLEU[35], ROUGE-L[27], METEOR[4]) and semantic similarity (BERTScore[52]). Across all five models, EyeLayer achieves consistent gains over fine-tuning baselines, with improvements up to 13.17% on BLEU-4, confirming that human attention signals enhance LLM performance across architectures.

This paper makes the following contributions:

- We propose a framework for integrating human cognitive priors into large language models for code summarization. Using eye-tracking data as transferable probabilistic priors, our approach establishes a bridge between human attention behavior and LLM-level attention formation.
- We design the *Multimodal Gaussian EyeLayer*, a lightweight, recommendation-like module that redistributes code embeddings through learnable Gaussian mixtures. This mechanism decouples gaze-informed redistribution from intrinsic attention weights, enabling scalable integration of sparse human signals into billion-parameter LLMs without disrupting pretrained representations.
- We conduct a systematic evaluation across five LLMs spanning both encoder-only and decoder-only architectures, demonstrating consistent improvements on the CodeXGLUE benchmark and strong transferability of learned attention priors to unseen code.
- To facilitate reproducibility and foster future research, we release our implementation scripts and datasets at [URL](#).

In the rest of this paper, Section 2 presents the background of eye-tracking in program comprehension and probabilistic attention modeling. Section 3 introduces the design and implementation details of the proposed *EyeLayer* architecture. Section 4 details the experimental setup. Section 5 analyze the results. Section 6 discusses potential threats to validity. Section 7 provides a broader discussion of findings and implications. Section 8 reviews related work. Finally, Section 9 concludes the paper and outlines directions for future research.

2 Background

Human gaze behavior offers empirical insight into how developers comprehend code, while probabilistic attention provides a principled way to model such focus computationally. This section reviews key findings from eye-tracking studies and links them to Gaussian-based attention formulations that inspire our EyeLayer design.

2.1 Eye-tracking for Program Comprehension

Eye-tracking has become a rigorous method for examining cognitive processes in software engineering research, particularly in understanding how developers read and comprehend source code [17, 40]. By capturing gaze behavior, eye-tracking enables the quantitative analysis of attention allocation and processing effort with high temporal precision. In software engineering, this relationship is particularly relevant because program comprehension, like natural language reading, involves the incremental interpretation of complex visual and semantic structures [41]. Fixation-based metrics provide a means to infer where and when developers engage in information processing, distinguishing meaningful cognitive activity from mere visual transitions represented by saccades [39].

The theoretical basis for interpreting gaze data originates from cognitive psychology, most notably the work of Just and Carpenter [23]. Their eye–mind assumption states that the duration of a fixation, the period of relative ocular stability directly reflects the time required for cognitive processing. This principle established fixations as a reliable indicator of comprehension effort in reading, linking visual attention to linguistic and semantic processing. Empirical evidence shows that fixations occupy the vast majority of viewing time during code reading, emphasizing their role as the fundamental unit of analysis for understanding comprehension behavior [40, 41]. Overall, fixation analysis offers a direct and interpretable connection between observable gaze patterns and the underlying cognitive mechanisms of program understanding, making eye-tracking a valuable empirical approach for investigating how developers read, reason about, and make decisions based on source code.

2.2 Probabilistic Attention and Cognitive Priors

Transformer attention can be framed probabilistically, with weights parameterized as continuous distributions over positions. Gaussian parameterizations offer a simple and interpretable form: a mean for focus location and a variance for spread. Representative studies show concrete uses of such priors. Chorowski et al. introduced Gaussian-shaped attention for sequence-to-sequence alignment in speech recognition [8]. Cordonnier et al. analyzed self-attention and showed that learned patterns relate closely to Gaussian-like kernels over relative positions [10]. You et al. further reported that hard-coded Gaussian windows can match the performance of fully learned attention in machine translation, indicating that Gaussian structure can serve as an effective bias [49]. To allow multiple foci, Graves modeled attention as a mixture of Gaussians in recurrent architectures, capturing multi-modal alignments with learnable centers and spreads [19].

This probabilistic view aligns with findings from eye-tracking. Studies in software engineering report localized and selective fixations during code reading [7, 42]. Such fixation maps are commonly summarized as peaked distributions over spatial locations. Neural models inspired by selective vision, such as DRAW, use parameterized Gaussian filters to realize differentiable focus regions [20]. These results motivate representing model attention with Gaussian or mixture forms when human-like focus is desirable.

Guided by this evidence, our EyeLayer treats attention as a learnable mixture with sparse mode selection. The formulation provides

233 an interpretable parameter space (centers, spreads, and weights)
 234 consistent with probabilistic attention and with observed fixation
 235 patterns in code comprehension. This connects a statistical prior on
 236 attention with cognitively grounded signals in a single mechanism.
 237

238 3 Methodology

240 Our training employs a carefully designed dual-dataset strategy that
 241 separates the primary code summarization task from the auxiliary
 242 eye-tracking alignment task, enabling learning from both large-
 243 scale code-summary pairs and sparse but cognitively grounded
 244 attention signals. Figure 1 provides an overview of our complete
 245 approach.

247 3.1 Datasets and Preprocessing

249 Our training employs a carefully designed dual-dataset strategy that
 250 separates the primary code summarization task from the auxiliary
 251 eye-tracking alignment task, enabling learning from both large-
 252 scale code-summary pairs and sparse but cognitively grounded
 253 attention signals.

254 **Code Summarization Corpus.** We use the Java subset of the
 255 CodeXGLUE benchmark [29], a widely-adopted dataset containing
 256 Java methods paired with their corresponding docstring summaries
 257 extracted from open-source repositories. The dataset provides di-
 258 verse code patterns spanning different programming idioms, com-
 259 plexity levels, and documentation styles, enabling robust learning
 260 of the code-to-summary mapping across varied contexts.

261 **Eye-Tracking Corpus.** We derive the auxiliary alignment su-
 262 pervision from the EyeTrans corpus [55], which records the gaze
 263 behaviors of developers during controlled code comprehension
 264 tasks. Each sample links a Java method to its Abstract Syntax Tree
 265 (AST) and corresponding fixations that capture how programmers
 266 allocate attention across syntactic and semantic regions. A *fixa-
 267 tion* is defined as a spatially stable gaze lasting approximately
 268 100–300 ms [40], during which most visual information process-
 269 ing occurs [23]. Each fixation is localized on screen coordinates
 270 and mapped to its corresponding AST node, producing discrete yet
 271 cognitively grounded attention signals. These node-level fixation
 272 counts are then aligned to model-level subtoken representations
 273 through our three-stage matching pipeline described below, provid-
 274 ing precise human-derived supervision for multimodal alignment
 275 in the EyeLayer.

276 To effectively integrate these fixation-based signals into the
 277 model, we must reconcile the representational gap between the
 278 human gaze space and the model input space. The eye-tracking
 279 corpus encodes attention in the *AST node space*, identifying which
 280 syntactic constructs programmers focus on, whereas the multi-
 281 modal EyeLayer operates in the *subtoken space*, defined by byte-
 282 pair encoded tokens from the model tokenizer. This mismatch is
 283 non-trivial: (1) a single AST node like `BFSdistance` may split into
 284 multiple subtokens `[BFS, distance]`, (2) tokenization varies based
 285 on surrounding context and instruction templates, and (3) abstract
 286 AST nodes have no direct token correspondence. We address this
 287 through a three-stage alignment pipeline: first, we traverse the AST
 288 to extract concrete code elements; second, we apply context-aware
 289 tokenization matching the model’s instruction format; finally, we

291 use multi-strategy matching—exact matching for simple cases, con-
 292secutive aggregation for split tokens, and character offset estimation
 293 for complex constructs—to map AST nodes to subtoken indices.
 294 This pipeline achieves >98% mapping accuracy and enables us to
 295 transfer sparse node-level fixation counts to the dense subtoken
 296 representations required for attention supervision.

297 **Independent Data Sources.** To ensure clear supervision bound-
 298 aries, the two datasets are kept entirely independent. The code sum-
 299 marization corpus drives the primary generation objective, while
 300 the eye-tracking corpus contributes auxiliary alignment supervi-
 301 sion. They contain disjoint code samples, eliminating data leakage
 302 and ensuring that observed improvements stem from the integra-
 303 tion of human cognitive priors rather than exposure to additional
 304 labeled summaries.

306 3.2 Multimodal Gaussian EyeLayer

308 Our approach builds on the key insight that, during code compre-
 309 hension, programmers allocate attention unevenly across the code:
 310 they concentrate intensively on semantically critical regions while
 311 attending peripherally to contextual elements. This uneven distribu-
 312 tion can be viewed as a composition of several focus patterns, each
 313 representing a localized concentration of attention over the token
 314 sequence. To model this behavior, the **Multimodal Gaussian Eye-
 315 Layer** represents attention as a mixture of Gaussian components.
 316 Each component defines a focus region characterized by a center μ_k
 317 (semantic locus) and spread σ_k (contextual extent), while a sparse
 318 gating network determines how many such regions are needed for
 319 each code snippet. This formulation captures both concentrated
 320 and distributed focus within a unified probabilistic framework, al-
 321 lowing the model to adaptively modulate attention according to
 322 code structure and semantics.

323 The EyeLayer integrates into pretrained decoder-only transfor-
 324 mers (e.g., LLaMA, Qwen) through hook-based injection at an inter-
 325 mediate layer. During forward propagation, it intercepts hidden
 326 states \mathbf{H} , applies the EyeLayer transformation, and returns updated
 327 representations \mathbf{H}' to subsequent layers. This hook-based design
 328 preserves the causal structure of the base model while enriching its
 329 intermediate representations with human-aligned attention priors,
 330 as illustrated in Figure 2.

331 **3.2.1 Code-Level Embedding.** Before predicting Gaussian param-
 332 eters, the model first summarizes the overall semantic context of
 333 the input sequence. For hidden states $\mathbf{H} \in \mathbb{R}^{B \times L \times d}$ from an inter-
 334 mediate transformer layer, we apply an attention mask \mathbf{M}_{attn} and
 335 a special-token mask $\mathbf{M}_{\text{special}}$ to form $\mathbf{M} = \mathbf{M}_{\text{attn}} \odot (1 - \mathbf{M}_{\text{special}})$.
 336 When positional information is available, a decay factor $D_{p_i} = \gamma^{p_i}$
 337 ($\gamma = 0.95$) down-weights distant tokens. The code-level embedding
 338 is computed as:

$$\mathbf{e} = \frac{\sum_{i=1}^L M_i D_{p_i} \mathbf{H}_i}{\sum_{i=1}^L M_i + \epsilon}, \quad (1)$$

341 where ϵ is a small constant to avoid division by zero. The resulting
 342 vector $\mathbf{e} \in \mathbb{R}^d$ provides a compact semantic summary for mode
 343 prediction.

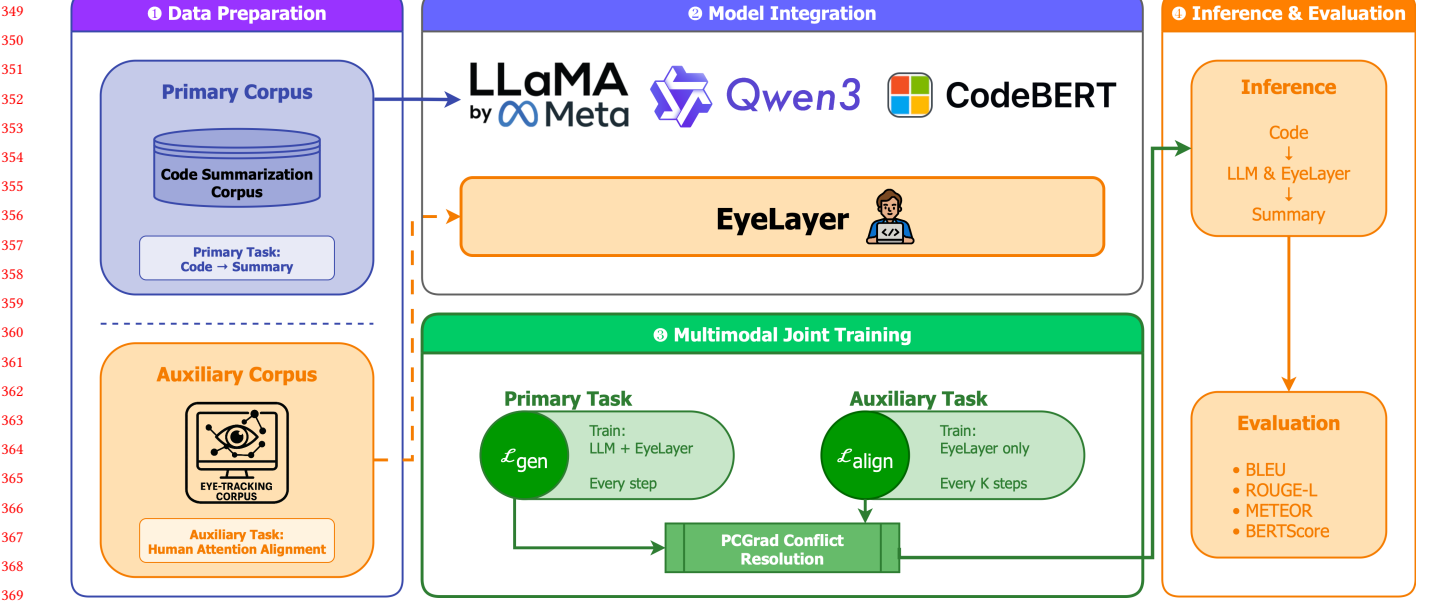


Figure 1: Overview of our joint training pipeline.

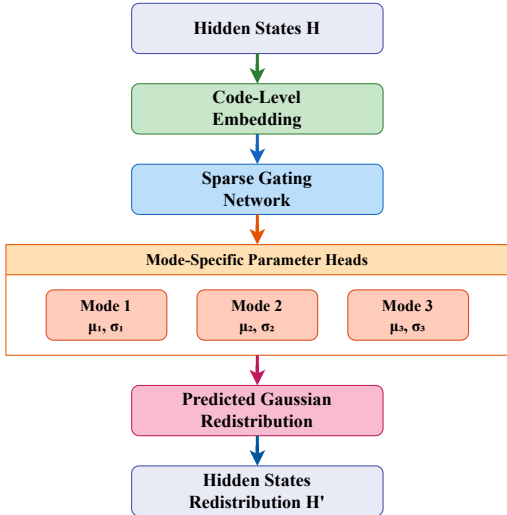


Figure 2: The Multimodal Gaussian EyeLayer architecture.

3.2.2 *Sparse Gating Mechanism.* To decide how many Gaussian components should be activated for each code sequence, the EyeLayer uses a lightweight gating network that maps the code embedding e to a normalized weight vector $w \in \mathbb{R}^K$:

$$w = \text{softmax}(\mathbf{W}_2 \phi(\mathbf{W}_1 e + \mathbf{b}_1) + \mathbf{b}_2), \quad (2)$$

where $\phi(\cdot)$ is a non-linear activation, and $\mathbf{W}_1, \mathbf{W}_2, \mathbf{b}_1, \mathbf{b}_2$ are learnable projection and bias parameters. The softmax normalization ensures $\sum_k w^{(k)} = 1$, yielding interpretable mode activations that indicate the relative contribution of each Gaussian component. This

gating mechanism encourages sparse activation: simple functions tend to concentrate weight on a single mode, whereas more complex code distributes attention across multiple regions. Such adaptive allocation allows the model to adjust its focus continuously without introducing discrete decisions or additional supervision.

3.2.3 *Mode-Specific Parameterization.* Each active mode predicts its Gaussian parameters based on shared semantic features extracted from the same code embedding e . The shared representation is computed as:

$$\mathbf{h}_{\text{shared}} = \text{Dropout}(\text{LayerNorm}(\text{GELU}(\mathbf{W}_h e + \mathbf{b}_h))), \quad (3)$$

where \mathbf{W}_h and \mathbf{b}_h are learnable projection parameters. Each mode then applies lightweight linear heads:

$$\tilde{\mu}_k = \mathbf{w}_\mu^{(k)} \mathbf{h}_{\text{shared}} + b_\mu^{(k)}, \quad (4)$$

$$\tilde{\sigma}_k = \mathbf{w}_\sigma^{(k)} \mathbf{h}_{\text{shared}} + b_\sigma^{(k)}, \quad (5)$$

where $\tilde{\mu}_k$ and $\tilde{\sigma}_k$ are raw predictions for the center and spread of the k -th Gaussian component. Predictions are constrained to $\mu_k \in [0, L-1]$ and $\sigma_k \in [\sigma_{\min}, L/2]$ to ensure valid ranges. Centroid biases are initialized to cover early, middle, and late regions of the sequence to promote spatial diversity during early training.

3.2.4 *Gaussian Mixture Construction.* The final attention distribution is formed as a weighted mixture of $K=3$ Gaussian components:

$$P(i) = \sum_{k=1}^K w^{(k)} \frac{\exp\left(-\frac{(i-\mu_k)^2}{2\sigma_k^2}\right)}{\sum_{j=1}^L \exp\left(-\frac{(j-\mu_k)^2}{2\sigma_k^2}\right)}, \quad (6)$$

where $P(i)$ denotes the predicted attention probability for token position i in a sequence of length L . Each token position corresponds to a code token aligned with an AST node, thus representing a specific

465 syntactic or semantic unit in the source code. $w^{(k)}$ is the normalized
 466 weight of the k -th mode, and the denominator ensures each
 467 Gaussian is properly normalized over all token positions. Smaller σ_k
 468 values produce sharper, concentrated peaks representing focused
 469 reading, whereas larger σ_k values yield broader distributions that
 470 capture peripheral attention. The resulting mixture $P(i)$ forms a
 471 smooth, interpretable, and differentiable attention distribution that
 472 aligns with empirical human fixation patterns and supports end-
 473 to-end optimization. The resulting distribution ($P(i)$) serves as the
 474 human-aligned attention prior used in the subsequent causal-aware
 475 redistribution stage (Section 3.3).

3.3 Causal-Aware Attention Redistribution

477 Integrating human-guided attention into decoder-only transform-
 478 ers predicted by the EyeLayer requires preserving their causal au-
 479 toregressive dependency. Unlike encoder-based models that per-
 480 mit bidirectional attention, decoder-only architectures must main-
 481 tain strict left-to-right information flow so that each token pre-
 482 diction depends only on preceding context. Directly modifying
 483 attention weights or masks would break this constraint and dis-
 484 rupt key-value caching during generation. To address this, we im-
 485 plement *causal-aware redistribution*, which injects human-aligned
 486 guidance through residual perturbations of hidden states rather
 487 than altering attention masks. The perturbation is shaped by the
 488 Gaussian attention distribution predicted by the EyeLayer, enabling
 489 soft alignment toward human-attended regions while fully preserv-
 490 ing causality. The mechanism proceeds in three stages: (1) low-rank
 491 transformation for compact perturbation generation, (2) attention-
 492 guided weighting for cognitively informed modulation, and (3)
 493 adaptive gating for dynamic integration control.

494 **3.3.1 Low-Rank Transformation.** To prevent overfitting on lim-
 495 ited eye-tracking data, perturbations are generated through a low-
 496 rank bottleneck. Given hidden states $\mathbf{H} \in \mathbb{R}^{B \times L \times d}$ from a target
 497 transformer layer, we first down-project and then reconstruct the
 498 representations:

$$Z = \text{ReLU}(\mathbf{H}\mathbf{W}_{\text{down}}), \quad (7)$$

$$\Delta\mathbf{H}_{\text{base}} = Z\mathbf{W}_{\text{up}}, \quad (8)$$

505 where $\mathbf{W}_{\text{down}} \in \mathbb{R}^{d \times r}$ and $\mathbf{W}_{\text{up}} \in \mathbb{R}^{r \times d}$ are learnable projections
 506 with rank $r \ll d$. This factorization requires only $2dr$ parameters
 507 instead of d^2 , providing a $64\times$ reduction when $r = 16$ for $d = 2048$,
 508 while retaining sufficient representational capacity.

510 **3.3.2 Attention-Guided Weighting.** The perturbation is reweighted
 511 according to the predicted Gaussian attention distribution, empha-
 512 sizing regions that align with human gaze. For each sample b and
 513 token position i , we compute:

$$\tilde{\Delta}\mathbf{H}_{b,i} = \lambda P_b(i) \Delta\mathbf{H}_{\text{base},b,i} \odot A_i, \quad (9)$$

517 where $P_b(i)$ denotes the mixture-based attention probability at
 518 position i , λ is a learnable scaling coefficient, $A_i \in \{0, 1\}$ marks
 519 valid token positions, and \odot represents element-wise multiplication.
 520 Since redistribution operates on hidden representations rather than
 521 attention masks, causal self-attention remains intact: each token

523 still attends only to past positions ($j \leq i$), while its representa-
 524 tion is softly modulated toward human-attended regions. Gradient
 525 clipping is applied to ensure numerical stability.

526 **3.3.3 Adaptive Gating and Integration.** Finally, an adaptive high-
 527 way gate controls the strength of human-guided perturbation for
 528 each sample. A scalar gate value $g_b \in [0, g_{\text{max}}]$ is computed as:

$$g_b = g_{\text{max}} \sigma(\text{MLP}([\tilde{\mathbf{h}}_b; \mathbf{f}_b])), \quad (10)$$

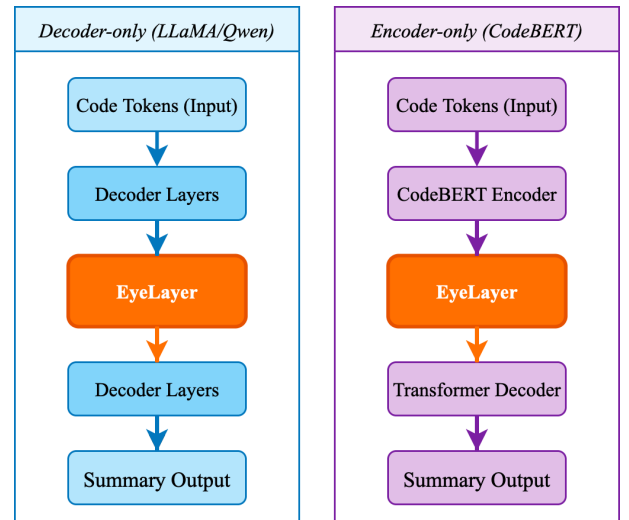
531 where $\tilde{\mathbf{h}}_b = \frac{1}{L} \sum_{i=1}^L \mathbf{H}_{b,i}$ is the mean-pooled hidden state (layer-
 532 normalized before concatenation), \mathbf{f}_b encodes global statistics of
 533 the attention distribution (e.g., entropy, maximum probability, and
 534 in the multimodal case, mode count and weight entropy), and $\sigma(\cdot)$
 535 is the sigmoid activation. The MLP is initialized with a negative
 536 bias to encourage conservative gating during early training. The
 537 final hidden states are obtained via residual integration:

$$\mathbf{H}'_{b,i} = \mathbf{H}_{b,i} + \alpha g_b \tilde{\Delta}\mathbf{H}_{b,i}, \quad (11)$$

540 where α is a global scaling constant. When g_b is small, the EyeLayer
 541 exerts minimal influence; as g_b increases, stronger redistribution
 542 occurs, enabling adaptive incorporation of human attention signals
 543 while preserving the model's pretrained representations.

3.4 Model Integration

544 The Multimodal EyeLayer integrates with transformer architectures
 545 through strategies that respect their information flow, as shown in
 546 Figure 3.



547 **Figure 3: Integration of the EyeLayer into transformer archi-
 548 tectures for code summarization.** Note that since CodeBERT
 549 is an encoder-only model, an auxiliary decoder is attached
 550 for sequence generation in the code summarization task.

553 **Decoder-Only Models (LLaMA, Qwen).** For autoregressive
 554 decoder-only architectures, the EyeLayer is injected at an inter-
 555 mediate transformer layer. During forward propagation, when the base
 556 model reaches the target layer, the hook intercepts hidden states \mathbf{H} ,
 557 applies the EyeLayer transformation, and returns enhanced repre-
 558 sentations \mathbf{H}' to subsequent layers. The predicted distribution $P(i)$

581 guides causal-aware attention redistribution (Section 3.3), which
 582 enforces that token i only attends to positions $j \leq i$ and preserves
 583 the decoder’s generation order.

584 **Encoder-Only Models (CodeBERT).** For encoder-only archi-
 585 tectures, the EyeLayer operates after CodeBERT and before the
 586 auxiliary decoder. CodeBERT processes the input code to produce
 587 contextualized hidden states H_{enc} , which are pooled to obtain a
 588 global code embedding that drives gating and mode prediction. The
 589 resulting $P(i)$ modulates H_{enc} via a non-causal low-rank perturba-
 590 tion over token positions; causal masking is not applied because
 591 the encoder is bidirectional. The decoder then cross-attends to the
 592 modulated encoder representations enriched with human-aligned
 593 attention priors.

594 3.5 Joint Training

595 After integrating the EyeLayer into the model architecture, we
 596 jointly train the system on the primary code summarization and
 597 auxiliary eye-tracking alignment tasks. This joint learning setup
 598 allows the model to balance large-scale textual supervision with
 599 sparse but cognitively grounded human signals. Formally, the over-
 600 all objective combines a generation loss \mathcal{L}_{gen} and an auxiliary
 601 alignment loss \mathcal{L}_{align} (defined in Section 4.3.2):

$$602 \mathcal{L}_{total} = \mathcal{L}_{gen} + \lambda_{align} \mathcal{L}_{align}, \quad (12)$$

603 where λ_{align} is a small weighting coefficient that ensures the align-
 604 ment supervision acts as a regularizer rather than dominating optimi-
 605 zation.

606 *3.5.1 Interleaved Training Schedule.* Because the two datasets dif-
 607 fer greatly in scale, with tens of thousands of code-summary pairs
 608 and only hundreds of eye-tracking samples, we adopt an inter-
 609 leaved training schedule to maintain stability. During each epoch,
 610 the model primarily trains on the summarization dataset, updat-
 611 ing parameters with \mathcal{L}_{gen} at every step. Every K steps (typically
 612 $K = 200$), a batch from the eye-tracking dataset is inserted, and Eye-
 613 Layer is optimized jointly on \mathcal{L}_{total} with gradient conflict handling
 614 described in Section 3.5.2. At the end of each epoch, we conduct
 615 a dedicated alignment sweep over the entire eye-tracking dataset
 616 while freezing the base model parameters, updating only the Eye-
 617 Layer components. This two-phase schedule maintains consistent
 618 exposure to the generation objective and provides sufficient gradi-
 619 ent signal for the EyeLayer through dedicated alignment phases,
 620 preventing the alignment objective from being overshadowed by
 621 the main summarization task.

622 *3.5.2 Projecting Conflicting Gradients (PCGrad).* Multi-task opti-
 623 mization often leads to conflicting gradient directions between
 624 objectives. In our setting, the EyeLayer parameters are influenced
 625 by both \mathcal{L}_{gen} and \mathcal{L}_{align} , which may occasionally compete. To
 626 reconcile these objectives, we employ **Projecting Conflicting**
 627 **Gradients (PCGrad)** [50], which detects negative cosine similarity
 628 between task gradients and removes the conflicting component
 629 through orthogonal projection. When gradients are aligned, both
 630 signals are preserved; when they diverge, PCGrad adjusts each
 631 gradient to retain only the non-conflicting directions. The final par-
 632 ameter update uses the mean of the projected gradients, ensuring
 633 that human-guided supervision complements rather than disrupts
 634 the main learning objective.

4 Experimental Setup

635 This section details the experimental configuration used to eval-
 636 uate the proposed Multimodal Gaussian EyeLayer. We describe (1)
 637 dataset construction for both code summarization and eye-tracking
 638 supervision, (2) models and training infrastructure, and (3) eval-
 639 uation metrics for summarization quality and human attention
 640 alignment. These components collectively establish the framework
 641 for answering the research questions presented in Section 5.

642 4.1 Datasets

643 **Code Summarization Dataset.** We use a subset of CodeXGLUE [29],
 644 derived from CodeSearchNet-Java, as the primary supervision source.
 645 To reduce training cost while preserving data diversity, we sample
 646 10% of the corpus, yielding 16,492 training pairs, 518 validation
 647 pairs, and 1,095 test pairs. Each instance consists of a Java method
 648 paired with its corresponding docstring summary extracted from
 649 open-source repositories.

650 **Eye-Tracking Dataset.** We adopt the EyeTrans corpus [55] for
 651 human attention supervision. The corpus involves fixation data
 652 from 27 programmers performing code summarization tasks. Each
 653 data point corresponds to a unique (developer, method) pair, cover-
 654 ing 64 unique functions across diverse Java projects. We obtain
 655 annotated samples with fixation sequences aligned to AST nodes.
 656 These samples provide sparse but cognitively grounded supervision
 657 for guiding attention redistribution.

658 4.2 Models and Training Infrastructure

659 We evaluate our Multimodal Gaussian EyeLayer across three repre-
 660 sentative transformer architectures spanning different scales and
 661 designs: LLaMA3.2-1B and LLaMA3.2-3B (decoder-only instruction-
 662 tuned models), Qwen3-1.7B and Qwen3-4B (decoder-only base
 663 model), and CodeBERT (encoder-only code model). Training and
 664 evaluation are conducted on a single NVIDIA L40S GPU (45GB
 665 VRAM), confirming that our approach remains computationally
 666 efficient while effectively incorporating human attention guidance.

667 4.3 Evaluation Metrics

668 *4.3.1 Code Summarization Metrics.* We evaluate generation quality
 669 using four widely adopted metrics:

- **BLEU** [35]: Computes modified n-gram precision with a
 670 brevity penalty to quantify lexical overlap with references.
- **ROUGE-L** [27]: Measures F1 based on the longest common
 671 subsequence, reflecting sequence-level similarity.
- **METEOR** [4]: Aligns words using exact, stem, and syn-
 672 onym matches with fragmentation penalties, emphasizing
 673 recall and paraphrase recognition.
- **BERTScore** [52]: Computes contextual embedding simi-
 674 larity to assess semantic alignment between candidate and
 675 reference texts.

676 *4.3.2 Attention Alignment Metrics.* To align model-predicted atten-
 677 tion with human fixation patterns while preserving multimodal
 678 diversity, we define:

$$679 \mathcal{L}_{align} = \mathcal{L}_{match} + \lambda_{sep} \mathcal{L}_{MSP}, \quad (13)$$

where $\mathcal{L}_{\text{match}}$ aligns each Gaussian mode with fixation data, and \mathcal{L}_{MSP} enforces spatial separation among active modes. The matching term is computed as $\mathcal{L}_{\text{match}} = \sum_{k=1}^K \tilde{w}^{(k)} \sum_t \lambda_t \mathcal{L}_t^{(k)}$, where $t \in \{\text{CAL, SML, CR, AUP}\}$ and $\tilde{w}^{(k)}$ is the normalized mode weight. Here $w^{(k)}$, μ_k , and σ_k denote the weight, center, and spread of the k -th Gaussian; $P_k(i)$ is its normalized probability at token position i ; $F(i)$ is the human fixation frequency; and ϵ is a small stability constant.

Centroid Alignment (CAL). $\mathcal{L}_{\text{CAL}}^{(k)} = \sqrt{(\mu_k - \mu_{\text{human}})^2 + \epsilon}$, where μ_{human} is the empirical fixation centroid. This term aligns each predicted attention center μ_k with human focus regions.

Spread Matching (SML). $\mathcal{L}_{\text{SML}}^{(k)} = \sqrt{(\sigma_k - \sigma_{\text{target}})^2 + \epsilon}$, where σ_{target} represents the observed fixation spread. It ensures each mode captures realistic human attention breadth.

Concentration Reward (CR). $\mathcal{L}_{\text{CR}}^{(k)} = 1 - (\sum_{i \in \mathcal{W}} P_k(i))^2$, where \mathcal{W} is a local window around attended tokens. This rewards probability mass concentrated near human fixation areas.

Anti-Uniform Penalty (AUP). $\mathcal{L}_{\text{AUP}}^{(k)} = \max(0, c - D_{\text{KL}}(U \| P_k))$, where $U(i) = 1/L$ is the uniform baseline, D_{KL} is KL divergence, and c is a small positive margin controlling the penalty strength. This term penalizes near-uniform distributions and promotes sharper attention focus.

Mode Separation (MSP). $\mathcal{L}_{\text{MSP}} = \sum_{k_1 < k_2} s_{k_1 k_2} \max(0, m - |\mu_{k_1} - \mu_{k_2}|)$, where $s_{k_1 k_2} = \mathbb{I}[w^{(k_1)} > \tau] \mathbb{I}[w^{(k_2)} > \tau]$, τ is the activation threshold, and m is the minimum distance between active mode centers. This term maintains spatial diversity across Gaussian components.

5 Experimental Results and Analysis

To evaluate the proposed Multimodal Gaussian EyeLayer, we address four research questions designed to quantify its effect on model performance, architectural behavior, and design components.

- **RQ1 – Does EyeLayer improve code summarization quality compared to standard supervised finetuning?**
- **RQ2 – How does the position of the EyeLayer within the transformer stack influence performance?**
- **RQ3 – How effectively does the EyeLayer generalize to encoder-only architectures?**
- **RQ4 – How does EyeLayer multimodal design contribute to performance?**

5.1 RQ1: Effectiveness Compared to SFT

RQ1 investigates whether integrating the proposed EyeLayer improves code summarization quality compared to standard supervised finetuning (SFT) without eye-tracking guidance. We evaluate four representative models: instruction-tuned (Llama3.2-1B/3B) and base (Qwen3-1.7B/4B).

As shown in Table 1, integrating EyeLayer leads to consistent gains across all models and evaluation metrics. Improvements appear in both lexical metrics (BLEU, ROUGE, METEOR) and semantic similarity (BERTScore), suggesting that cognitively inspired attention cues can guide the model toward more functionally meaningful code regions. For instruction-tuned models (Llama3.2-instruct), EyeLayer yields steady gains, particularly for the 1B model (+1.8 BLEU-4 / +1.9 METEOR). For base models (Qwen3), the improvement is

```

@Suppress("unchecked")
public static<T> R boolean tryScalarXMapSubscribe(
    Publisher<T> source,
    Subscriber<? super R> subscriber,
    Function<? super T, ? extends Publisher<? extends R>> mapper) {
    if (source instanceof Callable) {
        T t = ((Callable<T>) source).call();
        Publisher<? extends R> r = mapper.apply(t);
        if (r instanceof Callable) {
            R u = ((Callable<R>) r).call();
            subscriber.onSubscribe(new ScalarSubscription<R>(subscriber, u));
        } else {
            r.subscribe(subscriber);
        }
    }
}



With EyeLayer



Baseline



With EyeLayer



Baseline


```

Figure 4: Example from CodeXGLUE illustrating EyeLayer’s improvement over the baseline. Depict the inferred gaze-inspired attention across semantically related code regions.

larger in absolute terms, particularly for Qwen3-1.7B (ROUGE-L: +5.28, METEOR: +5.43), which indicates that models lacking instruction-level supervision may benefit more from additional attention prior.

The performance improvement suggests that EyeLayer subtly guides intermediate attention toward critical code regions that typically attract human gaze, thereby improving the quality of generated summary. The relatively larger gains observed in smaller models imply that supervision from the eye-tracking corpus provides a more informative inductive signal when model capacity and learned abstractions are limited. Larger models which already develop rich internal attention patterns, exhibit smaller yet consistent benefits. These observations collectively point to EyeLayer as a light but effective cognitive guidance mechanism, offering additional structure to models operating under supervision.

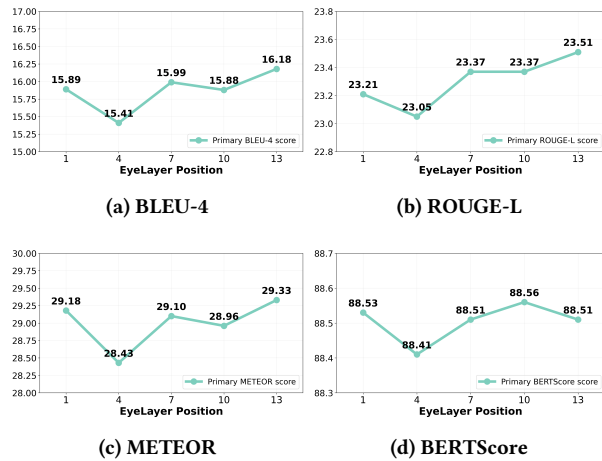
Figure 4 illustrates a representative example that demonstrates how EyeLayer enhances the generated summary. The baseline output, “Tries to create a scalar subscription for a given publisher,” captures only surface lexical cues, whereas EyeLayer produces a more accurate behavioral description, “Subscribes to the publisher using the mapper function as subscription handler.” Compared to the baseline, EyeLayer places stronger focus on the method declaration and variable declarations, which are semantically critical regions for capturing functional intent. This pattern resonates with the human attention dynamics reported by Karas et al. [24], where programmers most frequently alternate their gaze between method declarations and variable declarations during code comprehension. The correspondence suggests that EyeLayer internalizes similar focus tendencies without explicit gaze supervision during inference, enabling the model to generalize cognitive attention patterns that guide summarization toward semantically informative code regions.

RQ1 Summary. EyeLayer consistently improves summarization across all models, with larger gains in smaller or less supervised settings, showing that lightweight cognitive cues enhance semantic focus in code comprehension.

813 **Table 1: Performance comparison of baseline models and models with EyeLayer integration. Values in parentheses denote** 871
 814 **absolute improvement over the SFT baseline.** 872

816 Model	817 BLEU-4	818 ROUGE-L	819 METEOR	820 BERTScore
821 Llama3.2-1B	822 14.31	823 22.12	824 27.45	825 87.55
826 Llama3.2-1B + EyeLayer	827 16.18 (+1.87)	828 23.51 (+1.39)	829 29.33 (+1.88)	830 88.51 (+0.96)
831 Llama3.2-3B	832 15.64	833 24.57	834 29.83	835 88.29
836 Llama3.2-3B + EyeLayer	837 16.86 (+1.22)	838 25.25 (+0.68)	839 31.04 (+1.21)	840 88.72 (+0.43)
841 Qwen3-1.7B	842 13.36	843 21.39	844 26.60	845 86.04
846 Qwen3-1.7B + EyeLayer	847 15.12 (+1.76)	848 26.67 (+5.28)	849 32.03 (+5.43)	850 86.38 (+0.34)
851 Qwen3-4B	852 15.24	853 23.73	854 29.45	855 85.87
856 Qwen3-4B + EyeLayer	857 17.22 (+1.98)	858 25.30 (+1.57)	859 31.31 (+1.86)	860 86.27 (+0.40)

828 **5.2 RQ2: Effect of EyeLayer Insertion Position**



847 **Figure 5: Performance of Llama3.2-1B-Instruct when the Eye- 848 Layer is inserted at different transformer layers.**

851 We investigate how integration depth affects performance by 852 inserting the EyeLayer into different transformer layers of Llama3.2- 853 1B-Instruct (16 layers). Figure 5 shows the different metric trends 854 across positions.

855 Two clear patterns emerge: (1) performance improves toward 856 deeper layers and peaks at layer 13, and (2) a temporary drop appears 857 around layer 4. This trend aligns with the hierarchical roles of 858 transformer layers [32, 44]. Early layers capture lexical and syntactic 859 features, middle layers integrate contextual semantics, and later- 860 middle layers refine coherent representations for generation [13]. 861 The degradation at layer 4 likely reflects interference with unstable 862 intermediate encodings, as this stage is still reorganizing shallow 863 features into higher-level structures [53]. At layer 13, semantic 864 representations are largely formed yet remain adaptable. Injecting 865 human attention priors here allows modulation of semantic focus 866 without disrupting earlier composition, enhancing alignment with 867 meaningful program structures [32, 44].

868 Overall, these results highlight that the integration of cognitive 869 priors depends strongly on the model’s representational stage, with

878 later-middle layers providing the best balance between semantic 879 completeness and flexibility [13, 53].

886 **RQ2 Summary.** Performance peaks at later-middle layers, 887 where semantic representations are mature yet flexible, indicating 888 that cognitive priors are most effective after semantic 889 integration but before generation.

895 **5.3 RQ3: Generalization to Encoder-Only 896 Architectures**

898 Building on the results from decoder-only models (RQ1) and the 899 optimal integration depth analysis (RQ2), RQ3 examines whether 900 EyeLayer generalizes to encoder-only architectures, which differ 901 fundamentally in information flow and attention dynamics. We 902 evaluate this transferability using CodeBERT with the encoder- 903 side integration strategy described in Section 3.4. The results are 904 summarized in Table 2.

905 EyeLayer maintains consistent improvements across all metrics, 906 despite the architectural shift from decoder-only to encoder-only 907 models. The largest gain appears in METEOR (+1.83), indicating 908 enhanced semantic alignment and paraphrase understanding, both 909 of which rely on holistic code comprehension. The bidirectional 910 encoder benefits from modeling human-like focus over the entire code 911 context without causal masking, explaining its strong performance 912 on semantic metrics.

913 These results suggest that human attention patterns encode 914 architecture-invariant cues of semantic importance. Regardless of 915 whether information is processed autoregressively or bidirectionally, 916 guiding attention toward regions that typically attract human 917 gaze helps redistribute representational focus more effectively. The 918 multimodal Gaussian formulation accommodates these differences 919 without architectural redesign, demonstrating EyeLayer’s flexibility 920 and generalizability as a cognitively grounded attention module.

922 **RQ3 Summary.** EyeLayer generalizes well to encoder-only 923 models, confirming that human attention patterns provide 924 architecture-invariant cues for semantic importance and sup- 925 port flexible attention redistribution.

Table 2: CodeBERT performance with and without EyeLayer integration.

Model	BLEU-4	ROUGE-L	METEOR	BERTScore
CodeBERT	14.35	29.16	21.87	87.69
CodeBERT + EyeLayer	15.39 (+1.04)	30.70 (+1.54)	23.70 (+1.83)	88.30 (+0.61)

5.4 RQ4: Ablation Study on Multimodal Design

RQ4 investigates whether the multimodal Gaussian design, which models human attention through multiple distinct modes, provides advantages over simpler single mode alternatives.

To isolate the multimodal design’s contribution, we implement a simplified EyeLayer variant that predicts attention using a single Gaussian distribution rather than a mixture. This architecture removes the sparse gating network and mode-specific prediction heads, and instead directly predicts the global centroid μ and spread σ from the code-level embedding, while retaining all other components, including low-rank perturbation, attention-guided weighting, and adaptive highway gating. We evaluate single-mode EyeLayer at early and late layer positions on Llama3.2-1B-instruct.

Table 3 shows that multimodal EyeLayer consistently outperforms single-mode variants across all metrics. Single-mode configurations show limited improvements over baseline, with early layer achieving minimal gains and late layer showing inconsistent performance. In contrast, multimodal EyeLayer delivers substantial improvements. For example, at layer 13, multimodal design achieves BLEU-4: 16.18 versus single-mode’s 14.63 (+1.55), and METEOR: 29.33 versus 26.10 (+3.23), demonstrating clear advantages of modeling multiple attention modes.

The results support our hypothesis that human attention during code comprehension cannot be captured by a single Gaussian. A single-mode design can only represent one attention region, which forces a trade-off between narrow focus (small σ) and broad coverage (large σ), and thus fails to model multiple distinct areas of interest in complex functions. In contrast, the multimodal design enables sparse mode selection, where the gating network activates 1–3 modes adaptively based on code complexity. This allows the model to compose multiple attention patterns, such as scanning function signatures, following control flow, and inspecting implementation details. The substantial performance gains indicate that modeling diverse attention modes improves cognitive fidelity and justifies the added architectural complexity.

RQ4 Summary. Multimodal Gaussian design outperforms single-mode variants, demonstrating that modeling multiple attention modes better captures human gaze diversity and yields stronger semantic alignment.

6 Threats to Validity

There are two main threats to the validity of our work. First, our eye-tracking supervision derives exclusively from Java code comprehension, which may limit generalization to languages with different syntactic structures or paradigms. However, core code comprehension strategies are similar across languages. This implies that human attention patterns reflecting semantic importance may also transfer,

but further validation is needed for EyeLayer across diverse programming languages. Second, our evaluation relies on automatic metrics that may not fully correlate with human-perceived summary quality or practical developer productivity in real-world scenarios. We mitigate this threat by employing four complementary metrics (BLEU, ROUGE-L, METEOR, BERTScore) spanning lexical overlap and semantic similarity dimensions, validating across diverse model architectures (decoder-only and encoder-only), and conducting qualitative analysis demonstrating meaningful semantic improvements in generated summaries. All experiments used fixed random seeds to ensure reproducibility and minimize bias.

7 Discussion and Future Work

Scaling Eye-Tracking Supervision. Our results show that 625 sparse eye-tracking samples provide consistent benefits, suggesting that scaling supervision through data augmentation or large-scale collection could further improve performance. Richer supervision would enable more expressive EyeLayer architectures capturing finer-grained attention patterns.

Richer Cognitive Signals. Our approach uses only static fixation—aggregated attention intensity. Eye-tracking can contain additional information: saccade patterns (revealing information-seeking strategies), and attention switches (capturing dynamic shifts in cognitive focus). Incorporating these temporal and sequential signals has the potential to provide richer supervision.

Generalization to Software Engineering Tasks. While we focus on code summarization, many SE tasks fundamentally involve code comprehension: bug localization, code review, and program repair all require identifying semantically important regions. Human attention patterns should transfer across tasks as developers employ similar cognitive strategies regardless of end goal. EyeLayer’s effectiveness across both decoder-only and encoder-only architectures demonstrates its flexibility for integration into diverse models. However, future work should investigate whether attention patterns from code summarization tasks can transfer to other SE contexts, or whether collecting task-specific eye-tracking data yields stronger supervision signals.

Broader Implications. Beyond performance improvements, EyeLayer demonstrates grounding neural models in human cognitive processes rather than purely data-driven learning. This approach could enable more interpretable AI systems where models attend to code for reasons aligned with human reasoning, facilitating developer trust and effective human-AI collaboration as code intelligence tools become ubiquitous in development workflows.

8 Related Work

This section situates our work at the intersection of human-centered AI and automatic code summarization. We first review research that

Table 3: Ablation study comparing single-mode and multimodal EyeLayer designs on Llama3.2-1B.

Configuration	BLEU-4	ROUGE-L	METEOR	BERTScore
Baseline (SFT)	14.31	22.12	27.45	87.55
Single-mode (Early)	14.30	21.64	27.55	88.13
Single-mode (Late)	14.63	20.82	26.10	88.26
Multimodal (Late)	16.18	23.51	29.33	88.51

integrates cognitive and behavioral signals into software engineering models, emphasizing eye-tracking as a bridge between human and machine attention. We then discuss advances in code summarization, from transformer-based architectures to recent efforts incorporating human-like attention guidance.

8.1 Human-centered AI for Software Engineering

Human-centered AI for software engineering (SE) emphasizes aligning automated systems with human cognition and developer workflows. Empirical studies have shown that developers interact with AI assistants in complex ways: they often exhibit overconfidence while producing less secure code [36], alternate between acceleration and exploration modes depending on task certainty [6], and face persistent challenges in output validation and trust calibration [15, 26, 30]. Recent theoretical frameworks further characterize trust as a dynamic and multi-dimensional construct [9, 38], underscoring the need for models that are cognitively transparent and behaviorally adaptive.

Beyond behavioral analysis, recent research has sought to directly model cognitive processes underlying code comprehension. Early eye-tracking studies revealed that developer gaze patterns reflect semantic understanding during program reading [34, 37]. Building on this foundation, Bansal et al. [5] and Alakmeh et al. [2] predicted human attention from code structure and integrated gaze information to enhance summarization models. More recently, EyeTrans [55] and EyeMulator [54] incorporated gaze data into Transformer architectures, achieving measurable performance gains.

EyeLayer extends this research direction by being among the first to incorporate human cognitive signals into large language models. It leverages human attention as a transferable probabilistic prior, aiming for generalizable integration of human-like focus patterns across model architectures and tasks.

8.2 Automatic Code Summarization

The advent of large language models (LLMs) has catalyzed a paradigm shift in automatic code summarization, transitioning from traditional sequence-to-sequence architectures to transformer-based approaches that leverage extensive pre-training on code corpora. Early work such as Code2Seq [3] and retrieval-augmented methods [51] demonstrated that structural program representations and example-based retrieval can significantly enhance summary quality. The establishment of benchmarks like CodeXGLUE [28] standardized evaluation protocols and enabled systematic comparison across models and datasets. Building on these foundations, Shi et al. [43] identified key factors influencing neural summarization performance, while Gao et al. [16] and Fang et al. [12] explored

in-context and prompt-based learning to adapt general-purpose LLMs for code summarization. Empirical studies further revealed that moderately sized, fine-tuned models can rival or surpass much larger general-purpose LLMs when supervision effectively captures task semantics [46], emphasizing the centrality of the fine-tuning process in code-oriented adaptation.

Recent work has focused on improving efficiency, robustness, and interpretability in LLM-based summarization [46]. Su et al. [45] applied knowledge distillation to reduce computational costs, while Mastropaoletti et al. [31] proposed semantic-aware evaluation metrics to better assess summary fidelity. Virk et al. [47] exposed calibration deficiencies that undermine model reliability, and Mondal et al. [33] examined robustness to adversarial perturbations. Interpretability analyses further uncovered a persistent misalignment between model-generated attention and developer comprehension: Li et al. [25] showed that neural attention often diverges from code regions developers focus on, leading to summaries that are lexically fluent but semantically incomplete. This gap between surface-level correlations and true comprehension has motivated recent studies to augment fine-tuning with auxiliary behavioral cues such as eye-tracking, exemplified by EyeTrans [55], which guide transformer attention toward semantically salient regions.

EyeLayer continues this trajectory by strengthening the supervised fine-tuning of LLM-based summarization. Rather than redesigning model architectures or relying on heavy supervision, it introduces lightweight cognitive priors into the fine-tuning pipeline to steer attention toward functionally important code regions.

9 Conclusion

This work demonstrates that human cognitive patterns captured through eye-tracking can effectively enhance LLM-based code summarization. We introduced *EyeLayer*, a lightweight attention-augmentation module that integrates sparse human attention signals into LLMs through Multimodal Gaussian Mixture Models, enabling models to learn how developers naturally focus on semantically critical code regions during comprehension. Our evaluation across five models spanning different scales and architectures shows consistent improvements, validating that human expertise provides complementary signals that enhance LLM capabilities beyond what standard supervised fine-tuning achieves. Our methodology establishes a framework for incorporating human cognitive processes into LLMs for code comprehension, contributing to the development of more capable and interpretable developer tools as software systems continue to grow in complexity.

1161 **References**

1162 [1] Wasi Uddin Ahmad, Saikat Chakraborty, Baishakhi Ray, and Kai-Wei Chang. 2020. 1163 A Transformer-based Approach for Source Code Summarization. In *Proceedings 1164 of the 58th Annual Meeting of the Association for Computational Linguistics (ACL)*. 1165 [2] Tarek Alakmeh, David Reich, Lena Jäger, and Thomas Fritz. 2024. Predicting 1166 Code Comprehension: A Novel Approach to Align Human Gaze with Code Using 1167 Deep Neural Networks. *Proceedings of the ACM on Software Engineering* 1, FSE 1168 (July 2024), 1982–2004. doi:10.1145/3660795

1169 [3] Uri Alon, Shaked Brody, Omer Levy, and Eran Yahav. 2019. code2seq: Generating 1170 Sequences from Structured Representations of Code. arXiv:1808.01400 [cs.LG] 1171 <https://arxiv.org/abs/1808.01400>

1172 [4] Satanjeev Banerjee and Alon Lavie. 2005. METEOR: An Automatic Metric for MT 1173 Evaluation with Improved Correlation with Human Judgments. In *Proceedings 1174 of the ACL Workshop on Intrinsic and Extrinsic Evaluation Measures for Machine 1175 Translation and/or Summarization*, Jade Goldstein, Alon Lavie, Chin-Yew Lin, 1176 and Clara Voss (Eds.). Association for Computational Linguistics, Ann Arbor, 1177 Michigan, 65–72.

1178 [5] Aakash Bansal, Bonita Sharif, and Collin McMillan. 2023. Towards Modeling 1179 Human Attention from Eye Movements for Neural Source Code Summarization. 1180 *Proceedings of the ACM on Human-Computer Interaction* 7, ETRA (May 2023), 1–19. doi:10.1145/3591136

1181 [6] Shraddha Barke, Michael B. James, and Nadia Polikarpova. 2022. Grounded 1182 Copilot: How Programmers Interact with Code-Generating Models. doi:10.1145/3591136

1183 [7] Teresa Busjahn, Roman Bednarik, Andrew Begel, Martha Crosby, James H. Patterson, Carsten Schulte, Bonita Sharif, and Sascha Tamm. 2015. Eye Movements in Code Reading: Relaxing the Linear Order. In *2015 IEEE 23rd International Conference on Program Comprehension*. IEEE, Florence, Italy, 255–265. doi:10.1109/ICPC.2015.36

1184 [8] Jan K Chorowski, Dzmitry Bahdanau, Dmitriy Serdyuk, Kyunghyun Cho, and Yoshua Bengio. 2015. Attention-Based Models for Speech Recognition. In *Advances in Neural Information Processing Systems*, Vol. 28. Curran Associates, Inc.

1185 [9] Rudrajit Choudhuri, Bianca Trinkenreich, Rahul Pandita, Eirini Kalliamvakou, Igor Steinmacher, Marco Gerosa, Christopher Sanchez, and Anita Sarma. 2024. 1186 What Guides Our Choices? Modeling Developers' Trust and Behavioral Intentions 1187 towards GenAI. doi:10.48550/arXiv.2409.04099

1188 [10] Jean-Baptiste Cordonnier, Andreas Loukas, and Martin Jaggi. 2019. On the 1189 Relationship between Self-Attention and Convolutional Layers. In *International Conference on Learning Representations*.

1190 [11] Angela Fan, Beliz Gokkaya, Mark Harman, Mitya Lyubarskiy, Shubho Sengupta, 1191 Shin Yoo, and Jie M. Zhang. 2023. Large Language Models for Software Engineering: Survey and Open Problems. In *2023 IEEE/ACM International Conference 1192 on Software Engineering: Future of Software Engineering (ICSE-FoSE)*, 31–53. doi:10.1109/ICSE-FoSE59343.2023.00008

1193 [12] Minying Fang, Xing Yuan, Yuying Li, Haojie Li, Chunrong Fang, and Junwei Du. 2025. Enhanced Prompting Framework for Code Summarization with Large 1194 Language Models. *Proc. ACM Softw. Eng.* 2, ISSTA, Article ISSTA072 (June 2025), 1195 24 pages. doi:10.1145/3728949

1196 [13] Harshwardhan Partale, Ashish Kattamuri, Rahul Raja, Arpita Vats, Ishita Prasad, 1197 and Akshata Kishore Moharir. 2025. Disentangling Recall and Reasoning in 1198 Transformer Models through Layer-Wise Attention and Activation Analysis. doi:10.48550/arXiv.2510.03366

1199 [14] Zhangyu Feng, Daya Guo, Duyu Tang, Nan Duan, Xiaocheng Feng, Ming Gong, 1200 Linjun Shou, Bing Qin, Ting Liu, Daxin Jiang, and Ming Zhou. 2020. CodeBERT: 1201 A Pre-Trained Model for Programming and Natural Languages.

1202 [15] Yujia Fu, Peng Liang, Amjad Tahir, Zengyang Li, Mojtaba Shahin, Jiaxin Yu, and 1203 Jinfu Chen. 2025. Security Weaknesses of Copilot-Generated Code in GitHub 1204 Projects: An Empirical Study. doi:10.48550/arXiv.2310.02059

1205 [16] Shuzheng Gao, Xin-Cheng Wen, Cuiyun Gao, Wenxuan Wang, Hongyu Zhang, 1206 and Michael R. Lyu. 2023. What Makes Good In-Context Demonstrations for Code 1207 Intelligence Tasks with LLMs?. In *2023 38th IEEE/ACM International Conference 1208 on Automated Software Engineering (ASE)*. IEEE, 761–773. doi:10.1109/ase56229. 1209 2023.00109

1210 [17] Lisa Grabinger, Florian Hauser, Christian Wolff, and Jürgen Mottok. 2024. On 1211 Eye Tracking in Software Engineering. *SN Computer Science* 5, 6 (July 2024), 729. doi:10.1007/s42979-024-03045-3

1212 [18] Aaron Grattafori, Abhimanyu Dubey, Abhinav Jauhri, Abhinav Pandey, Abhishek 1213 Kadian, Ahmad Al-Dahle, Aiesha Letman, Akhil Mathur, and et al. 2024. The Llama 3 Herd of Models. doi:10.48550/arXiv.2407.21783

1214 [19] Alex Graves. 2014. Generating Sequences With Recurrent Neural Networks. 1215 doi:10.48550/arXiv.1308.0850

1216 [20] Karol Gregor, Ivo Danihelka, Alex Graves, Danilo Jimenez Rezende, and Daan 1217 Wierstra. 2015. DRAW: A Recurrent Neural Network For Image Generation. doi:10.48550/arXiv.1502.04623

1218 [21] Xinyi Hou, Yanjie Zhao, Yue Liu, Zhou Yang, Kailong Wang, Li Li, Xiapu Luo, 1219 David Lo, John Grundy, and Haoyu Wang. 2024. Large Language Models for 1220 Software Engineering: A Systematic Literature Review. arXiv:2308.10620 [cs.SE] 1221 <https://arxiv.org/abs/2308.10620>

1222 [22] Hamel Husain, Ho-Hsiang Wu, Tiferet Gazit, Miltiadis Allamanis, and Marc Brockschmidt. 2019. CodeSearchNet challenge: Evaluating the state of semantic 1223 code search. *arXiv preprint arXiv:1909.09436* (2019).

1224 [23] Marcel Adam Just and Patricia A Carpenter. [n. d.]. A Theory of Reading: From 1225 Eye Fixations to Comprehension. ([n. d.]).

1226 [24] Zachary Karas, Aakash Bansal, Yifan Zhang, Toby Li, Collin McMillan, and Yu 1227 Huang. 2024. A Tale of Two Comprehensions? Analyzing Student Programmer 1228 Attention during Code Summarization. *ACM Trans. Softw. Eng. Methodol.* 33, 7, 1229 Article 193 (Aug. 2024), 37 pages. doi:10.1145/3664808

1230 [25] Jiliang Li, Yifan Zhang, Zachary Karas, Collin McMillan, Kevin Leach, and Yu 1231 Huang. 2024. Do Machines and Humans Focus on Similar Code? Exploring 1232 Explainability of Large Language Models in Code Summarization. In *Proceedings 1233 of the 32nd IEEE/ACM International Conference on Program Comprehension (Lisbon, 1234 Portugal) (ICPC '24)*. Association for Computing Machinery, New York, NY, USA, 1235 47–51. doi:10.1145/3643916.3644434

1236 [26] Jenny T. Liang, Chenyang Yang, and Brad A. Myers. 2023. A Large-Scale Survey 1237 on the Usability of AI Programming Assistants: Successes and Challenges. doi:10. 1238 48550/arXiv.2303.17125

1239 [27] Chin-Yew Lin. 2004. ROUGE: A Package for Automatic Evaluation of Summaries. 1240 In *Text Summarization Branches Out*. Association for Computational Linguistics, 1241 Barcelona, Spain, 74–81.

1242 [28] Shuai Lu, Daya Guo, Shuo Ren, Junjie Huang, Alexey Svyatkovskiy, Ambrosio 1243 Blanco, Colin Clement, Dawn Drain, Daxin Jiang, Duyu Tang, Ge Li, Lidong Zhou, 1244 Linjun Shou, Long Zhou, Michele Tufano, Ming Gong, Ming Zhou, Nan Duan, 1245 Neel Sundaresan, Shao Kun Deng, Shengyu Fu, and Shujie Liu. 2021. CodeXGLUE: 1246 A Machine Learning Benchmark Dataset for Code Understanding and Generation. 1247 (2021). arXiv:2102.04664 [cs.SE] <https://arxiv.org/abs/2102.04664>

1248 [29] Shuai Lu, Daya Guo, Shuo Ren, Junjie Huang, Alexey Svyatkovskiy, Ambrosio 1249 Blanco, Colin B. Clement, Dawn Drain, Daxin Jiang, Duyu Tang, Ge Li, Lidong 1250 Zhou, Linjun Shou, Long Zhou, Michele Tufano, Ming Gong, Ming Zhou, Nan 1251 Duan, Neel Sundaresan, Shao Kun Deng, Shengyu Fu, and Shujie Liu. 2021. CodeXGLUE: 1252 A Machine Learning Benchmark Dataset for Code Understanding and Generation. 1253 *CoRR* abs/2102.04664 (2021).

1254 [30] Yunbo Lyu, Zhou Yang, Jieke Shi, Jianming Chang, Yue Liu, and David Lo. 2025. 1255 "my Productivity Is Boosted, but ..." Demystifying Users' Perception on AI Coding 1256 Assistants. doi:10.48550/arXiv.2508.12285

1257 [31] Antonio Mastropaoletti, Matteo Ciniselli, Massimiliano Di Penta, and Gabriele 1258 Bavota. 2024. Evaluating Code Summarization Techniques: A New Metric and 1259 an Empirical Characterization. In *Proceedings of the IEEE/ACM 46th International 1260 Conference on Software Engineering (Lisbon, Portugal) (ICSE '24)*. Association for 1261 Computing Machinery, New York, NY, USA, Article 218, 13 pages. doi:10.1145/ 1262 3597503.3639174

1263 [32] Jack Merullo, Carsten Eickhoff, and Ellie Pavlick. 2025. Talking Heads: 1264 Understanding Inter-Layer Communication in Transformer Language Models. 1265 doi:10.48550/arXiv.2406.09519

1266 [33] Debanjan Mondal, Abhilasha Lodha, Ankita Sahoo, and Beena Kumari. 2023. 1267 Robust Code Summarization. In *Proceedings of the 1st GenBench Workshop on (Benchmarking) Generalisation in NLP*, Dieuwke Hupkes, Verna Dankers, Khuyagbaatar 1268 Batsuren, Koustuv Sinha, Amirhossein Kazemnejad, Christos Christodoulopoulos, 1269 Ryan Cotterell, and Elia Bruni (Eds.). Association for Computational Linguistics, 1270 Singapore, 65–75. doi:10.18653/v1/2023.genbench-1.5

1271 [34] Matteo Paltenghi and Michael Pradel. 2021. Thinking like a Developer? Comparing 1272 the Attention of Humans with Neural Models of Code. In *2021 36th IEEE/ACM 1273 International Conference on Automated Software Engineering (ASE)*. IEEE, 1274 Melbourne, Australia, 867–879. doi:10.1109/ase51524.2021.9678712

1275 [35] Kishore Papineni, Salim Roukos, Todd Ward, and Wei-Jing Zhu. 2002. Bleu: 1276 A Method for Automatic Evaluation of Machine Translation. In *Proceedings of 1277 the 40th Annual Meeting of the Association for Computational Linguistics*, Pierre 1278 Isabelle, Eugene Charniak, and Dekang Lin (Eds.). Association for Computational 1279 Linguistics, Philadelphia, Pennsylvania, USA, 311–318. doi:10.3115/1073083. 1280 1073135

1281 [36] Neil Perry, Megha Srivastava, Deepak Kumar, and Dan Boneh. 2023. Do Users 1282 Write More Insecure Code with AI Assistants?. In *Proceedings of the 2023 ACM 1283 SIGSAC Conference on Computer and Communications Security*. ACM, Copenhagen, 1284 Denmark, 2785–2799. doi:10.1145/3576915.3623157

1285 [37] Paige Rodeghero, Collin McMillan, Paul W. McBurney, Nigel Bosch, and Sidney 1286 D'Mello. 2014. Improving Automated Source Code Summarization via 1287 an Eye-Tracking Study of Programmers. In *Proceedings of the 36th International 1288 Conference on Software Engineering*. ACM, Hyderabad India, 390–401. doi:10.1145/ 1289 2568225.2568247

1290 [38] Sadra Sabouri, Philipp Eibl, Xinyi Zhou, Morteza Ziyadi, Nenad Medvidovic, 1291 Lars Lindemann, and Souti Chattopadhyay. 2025. Trust Dynamics in AI-assisted 1292 Development: Definitions, Factors, and Implications. In *2025 IEEE/ACM 47th International 1293 Conference on Software Engineering (ICSE)*. IEEE, Ottawa, ON, Canada, 1294 1678–1690. doi:10.1109/ICSE55347.2025.00199

1295 [39] Zohreh Sharafi, Timothy Shaffer, Bonita Sharif, and Yann-Gaël Guéhéneuc. 2015. 1296 Eye-Tracking Metrics in Software Engineering. In *2015 Asia-Pacific Software 1297* <https://arxiv.org/abs/2308.10620>

1277 *Engineering Conference (APSEC)*. 96–103. doi:10.1109/APSEC.2015.53

1278 [40] Zohreh Sharifi, Bonita Sharif, Yann-Gaël Guéhéneuc, Andrew Begel, Roman Bednarik, and Martha Crosby. 2020. A Practical Guide on Conducting Eye Tracking Studies in Software Engineering. *Empirical Software Engineering* 25, 5 (Sept. 2020), 3128–3174. doi:10.1007/s10664-020-09829-4

1279 [41] Zohreh Sharifi, Zéphyrin Soh, and Yann-Gaël Guéhéneuc. 2015. A Systematic Literature Review on the Usage of Eye-Tracking in Software Engineering. *Information and Software Technology* 67 (Nov. 2015), 79–107. doi:10.1016/j.infsof.2015.06.008

1280 [42] Bonita Sharif and Jonathan I. Maletic. 2010. An Eye Tracking Study on camelCase and Under_score Identifier Styles. In *2010 IEEE 18th International Conference on Program Comprehension* 196–205. doi:10.1109/ICPC.2010.41

1281 [43] Ensheng Shi, Yanlin Wang, Lun Du, Junjie Chen, Shi Han, Hongyu Zhang, Dongmei Zhang, and Hongbin Sun. 2022. On the evaluation of neural code summarization. In *Proceedings of the 44th International Conference on Software Engineering*. ACM, 1597–1608. doi:10.1145/3510003.3510060

1282 [44] Oscar Skean, Md Rifat Arefin, Dan Zhao, Niket Patel, Jalal Naghiyev, Yann LeCun, and Ravid Shwartz-Ziv. 2025. Layer by Layer: Uncovering Hidden Representations in Language Models. doi:10.48550/arXiv.2502.02013

1283 [45] Chia-Yi Su and Collin McMillan. 2024. Distilled GPT for source code summarization. *Automated Software Engg.* 31, 1 (March 2024), 26 pages. doi:10.1007/s10515-024-00421-4

1284 [46] Weisong Sun, Yun Miao, Yuekang Li, Hongyu Zhang, Chunrong Fang, Yi Liu, Gelei Deng, Yang Liu, and Zhenyu Chen. 2025. Source Code Summarization in the Era of Large Language Models. arXiv:2407.07959 [cs.SE] <https://arxiv.org/abs/2407.07959>

1285 [47] Yuvraj Virk, Premkumar Devanbu, and Toufique Ahmed. 2025. Calibration of Large Language Models on Code Summarization. *Proc. ACM Softw. Eng.* 2, FSE, Article FSE130 (June 2025), 21 pages. doi:10.1145/3729400

1286 [48] An Yang, Anfeng Li, Baosong Yang, Beichen Zhang, Binyuan Hui, Bo Zheng, Bowen Yu, and et al. 2025. Qwen3 Technical Report. doi:10.48550/arXiv.2505.09388

1287 [49] Weiqiu You, Simeng Sun, and Mohit Iyyer. 2020. Hard-Coded Gaussian Attention for Neural Machine Translation. In *Proceedings of the 58th Annual Meeting of the Association for Computational Linguistics*, Dan Jurafsky, Joyce Chai, Natalie Schluter, and Joel Tetreault (Eds.). Association for Computational Linguistics, Online, 7689–7700. doi:10.18653/v1/2020.acl-main.687

1288 [50] Tianhe Yu, Saurabh Kumar, Abhishek Gupta, Sergey Levine, Karol Hausman, and Chelsea Finn. 2020. Gradient Surgery for Multi-Task Learning. doi:10.48550/arXiv.2001.06782

1289 [51] Jian Zhang, Xu Wang, Hongyu Zhang, Hailong Sun, and Xudong Liu. 2020. Retrieval-based neural source code summarization. In *Proceedings of the ACM/IEEE 42nd International Conference on Software Engineering* (Seoul, South Korea) (ICSE '20). Association for Computing Machinery, New York, NY, USA, 1385–1397. doi:10.1145/3377811.3380383

1290 [52] Tianyi Zhang, Varsha Kishore, Felix Wu, Kilian Q. Weinberger, and Yoav Artzi. 2020. BERTScore: Evaluating Text Generation with BERT. doi:10.48550/arXiv.1904.09675

1291 [53] Yang Zhang, Yanfei Dong, and Kenji Kawaguchi. 2024. Investigating Layer Importance in Large Language Models. In *Proceedings of the 7th BlackboxNLP Workshop: Analyzing and Interpreting Neural Networks for NLP*. Association for Computational Linguistics, Miami, Florida, US, 469–479. doi:10.18653/v1/2024.blackboxnlp-1.29

1292 [54] Yifan Zhang, Chen Huang, Yueke Zhang, Jiahao Zhang, Toby Jia-Jun Li, Collin McMillan, Kevin Leach, and Yu Huang. 2025. EyeMulator: Improving Code Language Models by Mimicking Human Visual Attention. doi:10.48550/arXiv.2508.16771

1293 [55] Yifan Zhang, Jiliang Li, Zachary Karas, Aakash Bansal, Toby Jia-Jun Li, Collin McMillan, Kevin Leach, and Yu Huang. 2024. EyeTrans: Merging Human and Machine Attention for Neural Code Summarization. *Proceedings of the ACM on Software Engineering* 1, FSE (July 2024), 115–136. doi:10.1145/3643732

1300 1335

1301 1336

1302 1337

1303 1338

1304 1339

1305 1340

1306 1341

1307 1342

1308 1343

1309 1344

1310 1345

1311 1346

1312 1347

1313 1348

1314 1349

1315 1350

1316 1351

1317 1352

1318 1353

1319 1354

1320 1355

1321 1356

1322 1357

1323 1358

1324 1359

1325 1360

1326 1361

1327 1362

1328 1363

1329 1364

1330 1365

1331 1366

1332 1367

1333 1368

1334 1369

1335 1370

1336 1371

1337 1372

1338 1373

1339 1374

1340 1375

1341 1376

1342 1377

1343 1378

1344 1379

1345 1380

1346 1381

1347 1382

1348 1383

1349 1384

1350 1385

1351 1386

1352 1387

1353 1388

1354 1389

1355 1390

1356 1391

1357 1392